Nuclear Physics A562 (1993) 365–388
North-Holland

NUCLEAR
PHYSICS A

Possible observation of medium effects using a pion correlation technique

J. Pluta [1], A. Rahmani, D. Ardouin, R. Lednicky [2], P. Stefański [3], H. Dąbrowski [4]

Laboratoire de Physique Nucléaire, IN2P3/CNRS et Université de Nantes, 2 rue de la Houssinière, 44072 Nantes Cedex 03, France

DIOGENE Collaboration

J.P. Alard [5], J. Augerat [5], N. Bastid [5], C. Cavata [6], P. Charmensat [6], P. Dupieux [5], P. Gorodetzky [7], J. Gosset [6], A. Le Merdy [6], D. L'Hôte [6], M.C. Lemaire [6], B. Lucas [6], J. Marroncle [5], G. Montarou [5], M.-J. Parizet [5], J. Poitou [6], D. Qassoud [5], O. Valette [6]

H.N. Agakishiev, V.G. Grishin [†]

Joint Institute for Nuclear Research, 141980 Dubna, Russian Federation

W. Bauer, P. Danielewicz, D. Klakow

National Superconducting Cyclotron Laboratory, Michigan State University, East Lansing, MI 48824-1321, USA

P. Schuck

Institut de Physique Nucléaire, Université de Grenoble, 53 avenue des Martyrs, 38026 Grenoble Cedex, France

Received 3 December 1992
(Revised 12 March 1993)

[†] Deceased in 1991.
Permanent address:
[1] Institute of Physics, Warsaw University of Technology, ul. Koszykowa 75, 00-662 Warsaw, Poland.
[2] Joint Institute for Nuclear Research, 141980 Dubna, Russian Federation.
[3] Institute of Nuclear Physics, ul. Kawiory 26a, 30-055 Kraków, Poland.
[4] Institute of Nuclear Physics, ul. Radzikowskiego 152, Kraków, Poland.
[5] Laboratoire de Physique Corpusculaire, Clermont Ferrand, Boîte Postale No. 45, 63170 Aubière, France.
[6] Département de Physique Nucléaire, Centre d'Etudes Nucléaires de Saclay, 91191 Gif-sur-Yvette Cedex, France.
[7] Centre de Recherches Nucléaires, Boîte Postale No. 20 CR, 67037 Strasbourg Cedex, France.
Correspondence to: Dr. D. Ardouin, Laboratoire de Physique Nucléaire, IN2P3/CNRS and Université de Nantes, 2 rue de la Houssinière, 44072 Nantes Cedex 03, France.

Abstract

Correlations of oppositely charged pions produced in interactions of protons and light nuclei with different nuclear targets are investigated. The invariant-mass distributions are analyzed in order to search for new conjectured nuclear effects. Strong and electromagnetic final-state interactions between pions and the Coulomb interaction between pions and the target nucleus are taken into account. An admixture of pion pairs coming from resonance decays is estimated. An enhancement in the low invariant-mass region is observed only for heavy target systems. A shadowing effect due to pion absorption inside the nuclear medium is considered as a possible source of this pattern. Azimuthal $\pi^+\pi^-$ correlations and pion yield dependence on the impact parameter, as well as transport calculations, seem to confirm this assumption.

Key words: NUCLEAR REACTIONS C, Nb, Pb (p, $\pi^+\pi^-$), $E=1.6$ GeV; H, C, Ta, (p, $\pi^+\pi^-$), $P=10$ GeV/c; H, C, Ta, (p and ^{12}C, $\pi^+\pi^-$), $P=4.2$ GeV/c; measured $\pi^+\pi^-$ invariant masses and correlation functions; Concluded pion absorption effects

1. Introduction

There exist indications that nuclear forces are mediated by the exchanged mesons and that these are present as virtual particles in nuclei [1]. After the first discoveries of the heavy mesons in the sixties, the one-boson exchange (OBE) model was developed [2] which assumed that the uncorrelated multi-pion exchange contribution was negligible as compared to the multi-pion resonances. Isoscalar–scalar mesons with mass around 400–800 MeV representing 2π S-wave resonances were assumed to account for the intermediate-range attraction of the nuclear force. Such resonances have never been identified experimentally as elementary particles [3].

More recent attempts to reconcile the meson-exchange theory with quantum chromodynamics are still far from being a quantitative and complete description, particularly for the intermediate-range NN interaction. It must be quoted here that a broad meson with $M \simeq 700$ MeV is required for a description of the $\pi\pi$ scattering in the framework of quark confinement models [4]. On the other hand the semi-microscopic theory of meson–meson interactions has lately been developed in quite some detail and with considerable success [5]. For example, the scalar–isoscalar phase shifts of $\pi^+\pi^-$ scattering can be very accurately reproduced up to 1400 MeV using a meson-exchange picture for the $\pi\pi$ interaction [6].

Modifications of hadron properties in nuclear matter have been recently studied [7–11] in order to emphasize the importance of medium effects. From these calculations, the possibility of bound two-pion pairs emerges from a build-up of the σ-strength above $2m_\pi$ which could affect the description of the intermediate-range NN interaction [12]. Nevertheless, such effects have not been clearly observed yet [10]. Indeed, the possible link of an experimental enhancement at low $\pi^+\pi^-$ invariant mass with the hypothetical existence of the σ-strength or strong s-wave interaction has been only studied with elementary reactions [13] where medium effects are absent.

Medium effects depend on the state of nuclear matter characterized by the values of density and temperature. Hypotheses of an equilibrated system, constant density and infinite nuclear matter are frequently assumed in the theoretical models [7–11]. In fact, these parameters depend on the space-time development of the interaction process. Other nuclear factors such as Pauli blocking, Fermi motion, binding energy etc. can also affect the results of theoretical calculations [14,15].

The mesonic degrees of freedom are strongly correlated with the excitation of the Δ-resonance and its propagation in the nuclear medium [16–20]. The properties of a Δ embedded in hot and dense nuclear matter are far from being described quantitatively [15,21]. Experimental results show a shift of the Δ-mass in nuclear collisions towards smaller values [22]. It turns out however, that a cascade which reflects fairly well this important feature of the Δ-excitation in nuclear matter cannot describe pion multiplicities in the same reaction [23]. This leads to the conclusion that not only the Δ-properties, but also the ΔN transition process, are modified by the nuclear environment [21,22,24]. Collective effects can also play an important role especially for highly compressed nuclear matter.

To test experimentally this multiparameter problem a great deal of data is clearly desired. In our studies we analyse the target-mass dependences of two-pion correlations fixing all the other experimental conditions in order to eliminate systematical uncertainties. The technique of the correlation function has been used in our analysis. It has the advantage of cleaning up many possible background effects in the observed coincidence spectra, enabling a higher sensitivity to any 2π correlation effect.

We have analyzed the $\pi^+\pi^-$ correlations resulting from the following data:
(1) p + C, p + Nb, p + Pb reactions at 1600 MeV projectile kinetic energy (Diogene Collaboration data [22,23]).
(2) ^{1}H, ^{2}H, ^{4}He, ^{12}C + propane at momentum 4.2 GeV/c per nucleon, p + Ta at 10 GeV/c (Dubna, propane bubble-chamber data [25,26]).

Although the analysis we present here comes from previous data, we must emphasize that none of the corresponding published results [22–25] ever looked at the $\pi^+\pi^-$ correlations. Rather, those works were devoted to other types of analyses like interferometry ($\pi^-\pi^-$ correlations) or Δ-resonance excitation (pπ coincidences).

The paper is organized as follows: in sect. 2 the experimental data will be presented. This will be followed by the correlation-data analysis from the Diogene detector and the propane bubble chamber. A discussion of the observed results will follow together with the presentation of various possible effects which could contribute to the observed pattern: electromagnetic background, final-state interactions, the known heavier resonances and medium effects.

2. The data

2.1. Diogene data

Diogene is the 4π-detector installed at the Saturne II synchrotron in Saclay. The synchrotron can deliver beams up to mass 40. The Diogene facility has been built to be able to perform exclusive measurements. An extensive description of this detector is given in ref. [27]. In this work we use the data from proton interaction with carbon, niobium and lead at a projectile kinetic energy of 1.6 GeV.

The Diogene detector is made of the pictorial drift chamber (PDC) and the plastic wall. Here in this paper we will present data from the PDC only. The PDC is a cylindrical drift chamber with an axis oriented parallel to the beam. The PDC is filled with an argon (86%)–propane (14%) mixture at a pressure of 4 atm. The central chamber of the Diogene detector is located inside a solenoid delivering a magnetic field of 1 T parallel to the beam direction (this value of the magnetic field results in a momentum resolution of 5% r.m.s. for a proton at 1 GeV/c of transverse momentum). The PDC measures light charged particles (π^+, π^-, p, d, t, ^{3}He and ^{4}He) in coincidence, emitted within the interval 20°–132° of polar angle in the laboratory. The general performances of the detector are those presented in the other results analyzed [22,23] with the same available experimental data. Concerning the charged pions we are interested in, the energy threshold (due to energy loss in the target and the beam pipe) is ~ 10 MeV corresponding to ~ 50 MeV/c particle momentum. The detector momentum resolution for pions detected in the PDC is about 20% (full width at half maximum) and 2°–4° for the azimuthal angle ϕ and the polar angle θ. The $e^{\pm}\pi^{\pm}$ separation is very good. Identified pions are not contaminated by electrons created by the gamma-ray conversion inside the target nor the beam pipe [23].

Before being further analyzed, each event is accepted if at least one π^- and one π^+ are within the polar angular range:

$$20° \leqslant \theta \leqslant 132° \tag{1}$$

and the low-energy thresholds are defined in the $(y, p_\perp/m)$ plane, where y denotes the rapidity of the particle and $p_\perp/m$ is the transverse momentum divided by the mass of the particle:

$$p_\perp/m \geqslant \begin{cases} 0.60 + 1.29y & (\text{if } y < 0) \\ 0.60 - 0.96y & (\text{if } y \geqslant 0). \end{cases} \tag{2}$$

2.2. Dubna data

We have performed an analysis of the experimental data obtained with the propane bubble chamber irradiated in the beams of light ions in the Laboratory of High Energies at the Joint Institute for Nuclear Research in Dubna. Propane (C_3H_8) gives one the possibility to investigate interactions with hydrogen and carbon targets. Another target (tantalum, $Z = 73$, $A = 181$) in the form of a 1 mm thick plate was placed inside the chamber. The following nuclei were used as projectiles: ^{1}H, ^{2}H, ^{4}He, ^{12}C at 4.2 GeV/c per nucleon and ^{1}H at 10 GeV/c. Again, the details concerning particle identification can be found with the other and previously published experimental results [25,26,28]. We will only present some resulting characteristics and performances relevant to our analysis.

Interactions with carbon have been selected from the sample of events recorded in liquid propane using charge conservation and kinematical criteria [29]. This method allows one to select with certainty about (70–80)% of the interactions with the carbon target. The remaining events consist of interactions with protons or peripheral carbon nucleons. It is important for the present analysis that the group of events selected as interactions with a carbon nucleus does not contain interactions with isolated protons. The applied selection procedure automatically enriches this sample by central-collisions events.

Interactions with a tantalum target have been selected by means of visual criteria. A small admixture of interactions with carbon, close to the tantalum plate can be present in our sample. An additional test has been made in the analysis assuming that the interaction point is located inside the plate. The possible contamination of the sample is then limited to a few percent.

Secondary particles were recorded in 4π geometry. The loss of pions emitted along the optical axes of the cameras is less than 3%. Pions were identified by their relative ionization, range in liquid propane and track curvature parameters. A minimal momentum for detected pions is about 70 MeV/c. All negative particles, other than identified electrons, were classified as π^- mesons. The admixture of misidentified electrons and negative strange particles among them does not exceed 5% and 1%, respectively. The maximum measured momentum of negative pions was not limited by the identification procedure. Positive pions were identified if their momenta were less than 1.0 GeV/c. In the momentum region (0.6–1.0) GeV/c some π^+ mesons were lost due to the identification ambiguities. For lower momenta, positive pions were well identified by their ionization. In the present analysis only well-identified particles were considered. The mean accuracy of the pion momentum and angle determination are about 10% and 0.5°, respectively. It gives the accuracy of the measurement of an effective mass of two pions from 6 MeV for masses close to $2m_\pi$, to about 40 MeV in the region of the ρ^0 resonance 700–800 MeV.

3. Analysis of the pion correlations

3.1. Definition of the correlation function

In order to extract information regarding two-pion correlations we have analyzed the density of $\pi^+\pi^-$ pairs in the phase space: $\rho(p_1, p_2) \sim \mathrm{d}N/\mathrm{d}p_1\,\mathrm{d}p_2$. The correlation function can be defined by the ratio:

$$R(p_1, p_2) = A\rho(p_1, p_2)/\rho_{\text{ref}}(p_1, p_2) \tag{3}$$

or the difference:

$$\Delta(p_1, p_2) = \rho(p_1, p_2) - B\rho_{\text{ref}}(p_1, p_2), \tag{4}$$

where p_1, p_2 are the pion momenta, $\rho_{\text{ref}}(p_1, p_2)$ is a reference density, A and B are the normalization constants.

The first formula is usually applied in analysis of the interference type correlations; the second one for the investigation of a resonance production. We have studied both of them, as the goal of our analysis is a search for new phenomena in the $\pi^+\pi^-$ system.

In the following analysis we build the correlation function from invariant-mass distributions of pion pairs. In order to find the relations between the correlation effects and the mass of a target nucleus we divide the total sample of the Dubna experimental material into three parts treated separately: interactions of light projectiles with an isolated nucleon, with a light (carbon) and with a heavy (tantalum) target. The Diogene data are also considered separately for the interactions of protons with light (carbon), medium (niobium) and heavy (lead) target nuclei.

3.2. Results from the Diogene data

The analysis of the experimental data has been performed in the same way for each of the reactions listed above.

The correlation function ΔN was calculated by the formula:

$$\Delta N = N(M_{\text{inv}}) - BN_{\text{ref}}(M_{\text{inv}}), \tag{5}$$

where N, N_{ref} are the numbers of pion pairs within a given interval of their invariant mass. The pions are taken from the same and different events, respectively; B is the normalization constant. Pions with momenta less than 500 MeV/c were taken. This cut was applied as positive pions with higher momenta cannot be well identified.

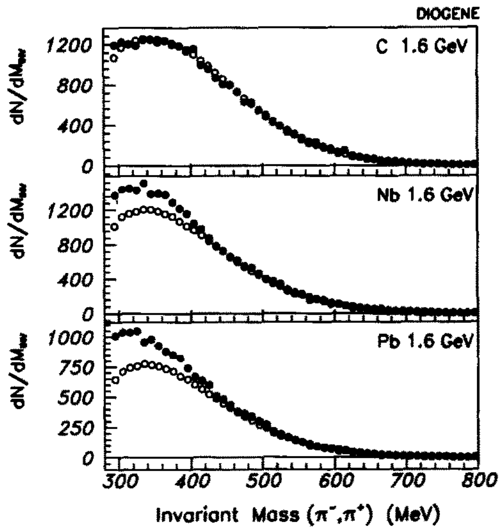

Fig. 1. Invariant-mass distributions of pion pairs from the Diogene data for three different targets: carbon (C), niobium (Nb) and lead (Pb). Open circles show background distribution, full circles show coincidence pairs.

Fig. 1 presents the invariant-mass distributions for the reactions of protons with C, Nb and Pb nuclei (black points). Corresponding reference distributions are shown by open circles. The normalization constant B was calculated to obtain: $\Sigma \Delta N = 0$ for $M_{\rm inv}$ greater than 500 MeV for each of the considered data sets. Fig.

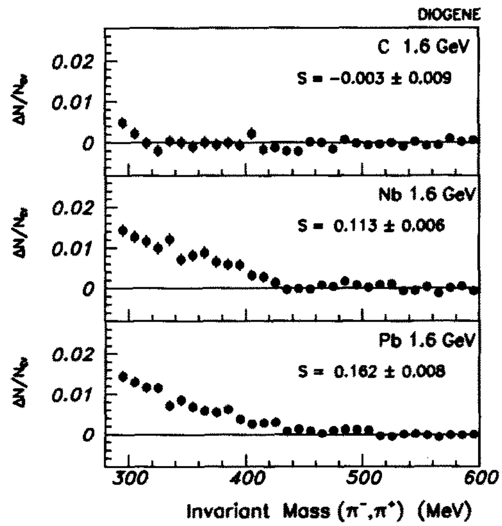

Fig. 2. The correlation function according to the definition (5) from the Diogene data divided by the total number of events. S denotes the integrated value of the function up to $M_{\rm inv} = 500$ MeV.

2 shows the corresponding correlation distributions as defined by the formula (5). The values of ΔN were divided by the number of events for each reaction considered, thus showing the number of correlated pion pairs per event. All pion pairs with an invariant mass less than 290 MeV have been rejected to avoid misidentification problems due to the modular structure of the Diogene detector.

A systematic change in the behavior of the correlation function can be observed when passing from light to heavier targets. For carbon nuclei the values of ΔN are close to zero with a small rise at low invariant mass. Small negative correlations are seen in the region of intermediate invariant mass. For the Nb and Pb targets, a qualitatively different form of the correlation distributions is seen. A positive correlation in the region of small invariant masses is clearly observed and is strongest for the Pb target. To express the correlation effect quantitatively we have integrated the ΔN spectrum for invariant masses less than 500 MeV. The corresponding results are displayed in fig. 2. For the carbon target the integrated correlation effect is negligible, while for the Nb and Pb targets it is far greater than the statistical errors.

3.3. Results from the Dubna data

The same procedure has been applied to the Dubna data. The results are presented in fig. 3. The coincidence distributions as well as the reference ones have been constructed separately for the samples of events coming from different projectiles. Due to the limited statistics we averaged the R-values over the ^{1}H, ^{2}H,

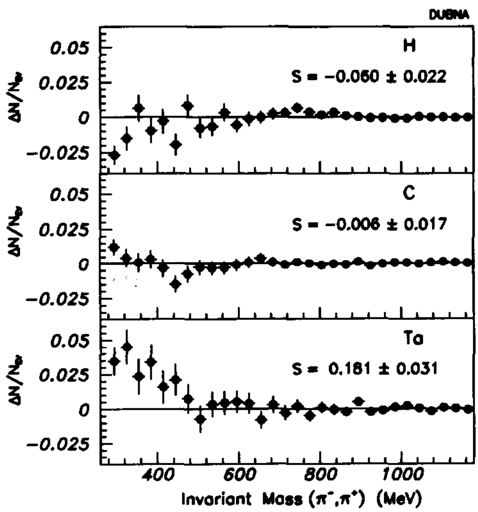

Fig. 3. Same as in fig. 2. from the Dubna data. The results from three targets: hydrogen (H), carbon (C) and tantalum (Ta) are shown.

^{4}H and ^{12}C projectiles for a given target and added the values of ΔN to reduce statistical errors. The above procedure is justified by the observation that for all groups of events with the same target, the correlation function is the same within the statistical uncertainty. Pions with the momenta less than 1000 MeV were taken for the analysis. The investigated phase space of pion production is thus reduced mainly to the target fragmentation region which is characterized by backward emission of pion pairs in the NN center-of-mass system.

The figure marked (H) shows the correlation distribution for events [25,26] which have been recorded in liquid propane and were not classified as interactions with carbon nuclei i.e. the interactions with hydrogen nuclei along with a part of peripheral interactions with carbon. The symbol (C) denotes the sample of events which passed the selection criteria for interaction with the carbon target. The figure marked (Ta) shows the same distribution obtained for the interactions with tantalum nuclei.

Despite the large statistical uncertainties some negative correlations can be observed in the region of small invariant mass for the interactions with proton-like target. Slight negative correlations which can be seen in the intermediate invariant-mass region for the carbon target are canceled by the positive ones in the low invariant-mass interval. A clear enhancement between the threshold and about 450 MeV is observed for the interactions with tantalum nuclei similarly to the effects seen from the Diogene data for Nb and Pb targets. A relatively great value of S for the tantalum target is a consequence of a greater pion multiplicity for the higher incident energy of the Dubna data.

3.4. Discussion

In order to find an origin of the observed correlations we consider below some effects which can be responsible for them. First there are some questions concerning the experimental technique and the method of correlation analysis.

Correlation effects between two emitted particles appear in a natural way due to phase-space restrictions, reaction dynamics, experimental acceptance etc. In order to look for additional correlation effects one has to take into account all the known sources of particle correlations. The detailed studies concerning this topic can be found in the papers devoted to the correlations of identical particles [30–32].

We have decided to use an event-mixing technique [33] to generate the reference (background) distribution. Particles selected for the mixing procedure were taken from the same class of events defined by its kinematical and dynamical characteristics [30]. The first condition which we have applied was to mix pions from events with the same pion multiplicity. In the case of hadron–nucleus collisions an important selection criterion is also the choice of reactions with the same impact parameter which determines the development of the interaction process. In our case the "proton-like multiplicity" [23] was used to select a sample of events with almost equal impact parameters for the Diogene data. The "number of participants" [28,34] was applied for the data from Dubna. It follows from the cascade calculations that these numbers can be used to perform such an impact parameter selection [23,34].

The interval of invariant mass $M_{inv} > 500$ MeV taken for the calculation of the normalization constant was chosen as a proper normalization for all the reactions considered. It turned out that the variation of this interval at the level of a few % does not affect the observed results as the correlation effects are limited to the invariant mass interval $M_{inv} < 450$ MeV. Above this value the coincidence and background distributions are practically the same as presented in fig. 1.

An example of trivial phase-space correlations can be seen in fig. 3. for the interactions with hydrogen target (protons). Negative correlations in the lower part of the invariant-mass distribution arise as a result of the four-momentum conservation. Indeed, this feature is destroyed in the event-mixing background [33] as far as a few particle system is concerned thus artificially depleting the correlation function in the region where these phase-space effects are expected to accumulate. We have proved by Monte Carlo simulations that in the case of elementary reactions in our energy region the pure phase-space effects give the negative correlations for small invariant masses. In the case of reactions with nuclear targets this effect will be substantially reduced by the secondary interactions which randomize the momenta of outgoing particles.

To check the sensivity of the background generation method to the different details of the applied mixing procedure we have tested different types of background distributions varying the number of mixed events and allowing for mixing between events with a different pion multiplicity. The cuts in pion energy were also made to look for the influence of possible effects due to the phase-space limitations. All these variations were not found to change the main trends of the observed correlations. Some more substantial effects will be considered below.

3.4.1. *Electromagnetic background*

The admixture of e^- and e^+ among charged pions can be relevant in the region of low effective mass where, due to phase-space limits, pion density is also reduced. The e^+e^- pairs come mainly from a π^0 decay with the subsequent γ-conversion close to the interaction point or from a creation of Dalitz pairs. Simultaneous misidentification of such e^+ and e^- corresponds to spurious $\pi^+\pi^-$ pairs with small invariant mass as the opening angle is very small in this case. This effect can therefore influence the shape of correlation distributions.

To estimate it, a kinematical simulation has been performed. Assuming that the π^0 momentum and angular distributions are similar to those of charged pions, a π^0 decay was simulated taking into account the experimental resolution. The e^+e^- pairs were then treated as pions and corresponding experimental errors were included into the simulation procedure. The idea of this test is to construct a π^- angular distribution in the rest frame of a pion pair with respect to the direction of the pair in the laboratory [13]. In the case of electrons, sharp peaks are seen in the forward and backward directions. About 70% of pairs are located within the interval: $|\cos\theta| > 0.975$. Analogous distributions were constructed for real pion pairs. It was found that the effect is seen outside the statistical dispersion limits only in the case of interactions with the tantalum target. Simple estimations confirm this observation. The probability of a γ-conversion from the π^0 decay in the tantalum plate is several times greater than the creation of a Dalitz pair or the conversion in propane close to the interaction point. The effect is seen only for small relative momenta in the $\pi\pi$ reference frame. Quantitative estimations were made for different intervals of effective mass distribution and the numbers of corresponding e^+e^- pairs were evaluated. These numbers were then subtracted from the effective mass distributions.

3.4.2. Pion–nucleus Coulomb interaction

It is natural to expect that the large positive charge of the emitting nucleus can affect the momentum difference between charged pions. The "external Coulomb corrections" were introduced in some analyses of interference correlations between identical pions [30]. The effects were found to be small, which is not surprising as the "momentum shift" has the same sign in this case. For unlike pions the situation is qualitatively different as the shift are in opposite directions. It can essentially affect the vector of the momentum difference.

We have evaluated the effect using the formulas of Gyulassy and Kaufmann [35] for static charge distribution thus correcting the data for the momentum shift:

$$\Delta \boldsymbol{k} = (\boldsymbol{k} - \boldsymbol{k}_0) = \pm \boldsymbol{k} \frac{Z\alpha\omega R}{\left(1 + (kR)^2\right)}, \tag{6}$$

where $\boldsymbol{k}_0$, $\boldsymbol{k}$ are the initial and final pion momenta, respectively; Z is the charge of the target nucleus, ω is the total pion energy, $\alpha = 1/137$; R is the mean inverse radius of the charged density:

$$R = \langle 1/r \rangle^{-1} = \sqrt{\tfrac{1}{2}\pi}\, r_0, \tag{7}$$

where $r_0 = \sqrt{\frac{1}{3}}\,\langle r^2 \rangle^{1/2}$ in the case of the gaussian distribution. The positive and negative signs correspond to π^+ and π^- mesons, respectively.

We have assumed here that important corrections arise from the Coulomb interactions between pions and the target nucleus. This assumption seems to be a good approximation for interactions of light projectiles with a heavy target nucleus.

The momentum shifts appear to be small in the case of the carbon target. For the interactions with heavy nuclei, the values of some tens MeV/c were obtained.

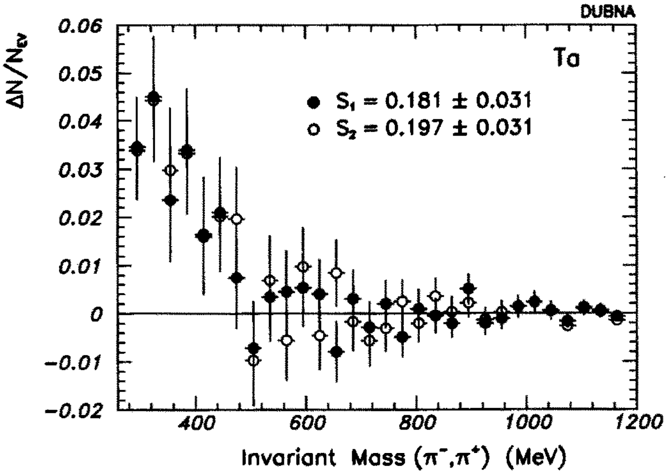

Fig. 4. The correlation function according to definition (5) for the tantalum target. The full circles show uncorrected values, the open ones shows values corrected for the Coulomb interactions between pions and a target nucleus. S denotes the integrated value of the function up to 500 MeV.

Consequently, one could expect a considerable influence of this effect on the shape of the correlation distributions. Fig. 4 shows the comparison of the original correlation distribution for the interactions with tantalum (the Dubna data) and that obtained after introducing the pion momentum corrections. Only a slight shift of the correlation effects towards a higher invariant mass is seen. This small shift does not change the global correlation effect.

Simple kinematical considerations show that the effects of the momentum changes in the single-particle scale are reduced when considering the momentum difference, Q, in the center-of-mass system of the pion pair. In the limit of small pion momenta the mean opening angle is relatively large so that opposite changes of the absolute values of pion momenta do not affect remarkably the absolute value of the momentum difference. For high values of pion momenta (small opening angles in the region where the effect is seen) the changes of this component of Q which is parallel to the pair velocity get reduced by the Lorentz transformation: $Q^2 = q_T^2 + Q_L^2/\gamma^2$, where γ is the Lorentz factor of a pion pair.

3.4.3. Final-state $\pi\pi$ interaction

The correlation function (CF) due to final-state interaction (FSI) of two unlike charged pions is defined as the ratio of the double inclusive momentum distribution to the one which would be observed in the case of no FSI effects. It is well known (see e.g. ref. [36]) that such a correlation function $R'(p_1, p_2)$ at nearby pion four-momenta p_1, p_2 is determined by the space-time distribution of the pion emission points and by the S-wave $\pi\pi$ scattering amplitude. We have calculated this CF according to formulas of ref. [36] (see also ref. [37]) assuming the gaussian

Table 1
The parameters in the expansion (8) of the $\pi\pi$ effective range functions [40]

I	a	b	c	d
0	0.26	0.25	0.35	−0.064
2	−0.028	−0.082	0.28	−0.0086

distribution of the space-time coordinates of the emission points characterized by the dispersions r_0^2 and τ_0^2, respectively. The dependence of the S-wave $\pi\pi$ scattering amplitude on the pion momentum k in the two-pion rest frame was parametrized using the representation of the S-wave amplitude f_I at fixed isospin $I=0,2$ given in ref. [38]. The corresponding effective range functions $g_I = 1/f_I + ik$ at $k < 500$ MeV/c are well approximated by the finite expansion taking into account a pole at negative energy:

$$g_I(k) = \frac{\sqrt{m_\pi^2 + k^2}}{a} \cdot \frac{1 + (c - a^2)(k/m_\pi)^2 + d(k/m_\pi)^4}{1 + (b/a + c)(k/m_\pi)^2}. \tag{8}$$

These expansions fit the experimental phase-shift data well and satisfy the constraints given by dispersion relations [39,40]. The parameters a_i, b_i, c_i, d_i are given in table 1.

In the case of no Coulomb interaction the $\pi^+\pi^-$ scattering amplitude is given by:

$$\tilde{f}_{\pi^+\pi^-} = \tfrac{2}{3} f_0 + \tfrac{1}{3} f_2. \tag{9}$$

We estimate the uncertainty of this amplitude at the level of 20%. The Coulomb interaction is switched on as usual [41]:

$$f_{\pi^+\pi^-}(k) = \left\{ \left[\frac{1}{\tilde{f}_{\pi^+\pi^-}(k)} + ik - \frac{2h(|ka_c|)}{a_c} \right] \Big/ A_c(k) - ik \right\}^{-1}, \tag{10}$$

where $a_c = -388$ fm is the Bohr radius of the $\pi^+\pi^-$ system; the h-function is defined in ref. [36] and

$$A_c(k) = \frac{2\pi}{ka_c} \left[\exp\left(\frac{2\pi}{ka_c} \right) - 1 \right]^{-1} \tag{11}$$

is the Coulomb penetration factor squared (the exponential function is the well known Gamow factor). In eq. (10) we neglect the change of the "neutral" amplitude $\tilde{f}_{\pi^+\pi^-}$ due to the Coulomb force (we expect this change to be less than

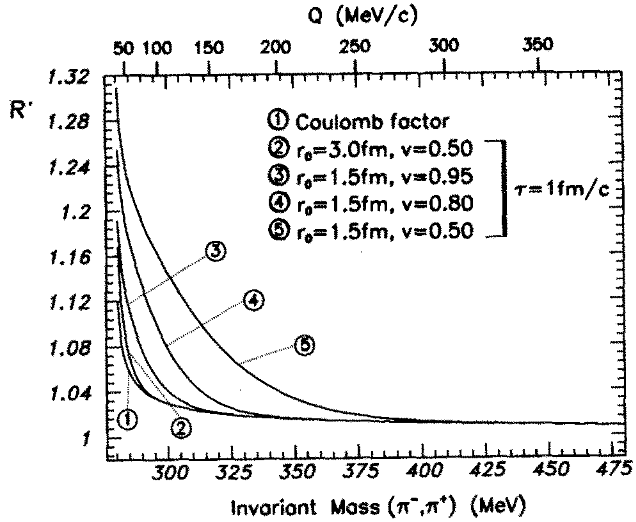

Fig. 5. The correlation function R' defined by the formula (12) for different values of a source radius (r_0) and velocity (v) as a function of the invariant mass of a pion pair (bottom scale) and the difference Q of pion momenta (upper scale).

10% even at $k=0$). We use the exact formulas (see ref. [37]) to calculate the Coulomb wave function outside the range of strong interaction; we note, however, that at $r_0 = \tau_0 = 1.5$ fm, the "point-like" approximation of ref. [36] overestimates the CF by only 2% or so.

In order to treat $R'(p_1, p_2)$ as a weighting factor for each event we have parametrized it in the form guessed on the basis of the analytical formulas of ref. [36]:

$$R'(p_1, p_2) = A_c(k)\left\{1 + \left[\left(b_1 + \frac{b_2}{\gamma}\right)Q^2 + b_3\right] \exp\left[-\left(b_4 + \frac{b_5}{\gamma}\right)Q^2\right]/\gamma\right\}, \tag{12}$$

where $Q = 2k$ and γ is the pion-pair Lorentz factor in the source rest frame.

Fig. 5 shows the dependence of the correlation function, R', on the value of Q (upper scale) and on the value of the two-pion invariant mass (lower scale). The chosen values of r_0 (1.5 and 3 fm) are close to the size of carbon and tantalum nuclei, respectively; (note that $r_0 = \sqrt{\frac{1}{3}}\langle r^2\rangle^{1/2}$ and the r.m.s. radii of the carbon and tantalum nuclei are: 2.52 and 5.38 fm, respectively [36,42]). The values of pion-pair velocities, v, correspond roughly to the minimal, mean and maximal values of the pair velocities as evaluated from the data. For the sake of comparison, the behavior of the Coulomb factor A_c is also shown. It can be seen that only for slow pions and a relatively small size of the pion emission volume, the

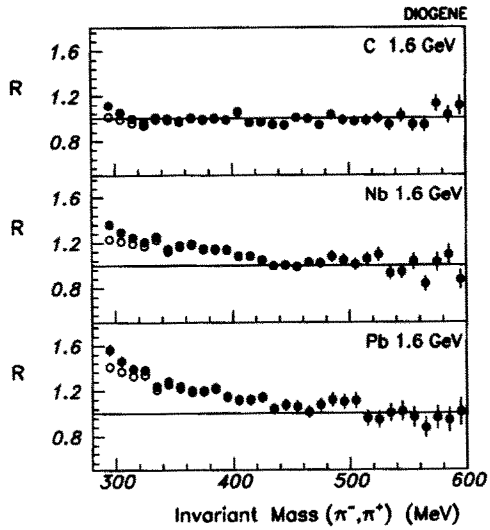

Fig. 6. The correlation function R defined by the formula (3) form the Diogene data. Full circles show uncorrected values, open ones show values corrected for the final-state interactions.

correlation function differs essentially form this simple approximation of the two-pion Coulomb interactions.

To estimate the contribution of the final-state interaction to the correlation effects which we have observed in the experimental data, the background distributions were weighted using the parameterization described above. A weighting by the Coulomb factor was also performed for comparison.

The results for the Diogene data are presented in fig. 6 as an example. This figure shows the correlation function in the form of a ratio (see formula 3) in accordance with the formalism of the FSI effects. The weighting factors were calculated assuming the size of pion emission volume corresponding to the size of a carbon nucleus ($r_0 = 1.5$ fm) for all the reactions considered. One can see that in the case of interactions with carbon the correlation effect appears mainly as a result of the final-state pion–pion interaction. For the interactions with niobium and lead nuclei the FSI effects change the shape of the correlation distributions a little in the region close to the threshold, leaving a major part of the distributions intact. Weighting only by the Coulomb factor gives a negligible correction in all the cases considered. The correction due to FSI, when assuming the size of pion emission volume corresponding to the size of the target nucleus, gives also negligible results for the niobium and lead target nuclei (see the curve 2 in fig. 5.) It is known, however, from the interferometry measurements [43] that a size of the pion emission region in high-energy nuclear collisions is more determined by the size of the smaller nucleus. Such a result was also obtained for the experimental data used here [45]. It should be also noted that by taking the size of the pion emission volume corresponding to the size of the smaller object, one estimates rather an upper limit of the FSI effects. It is well known that measured interference correlations usually give the smaller size of the volume responsible for a pion emission process as the greater one contributes with a narrower interference pattern [46].

3.4.4. Resonance decays

Among possible effects we have also examined the disintegration of the heavier known mesons. The $\omega^0 \to \pi^-\pi^+\pi^0$ (or γ) and $\eta^0 \to \pi^-\pi^+\pi^0$ (or γ) known channels [3] can contribute through π^- and π^+ coincidences to the observed data. We have simulated these decays assuming an isotropic emission in the resonance rest frame and folded these events with the experimental efficiency of the Diogene detector. It seems to be clear that the ω-meson cannot contribute significantly to the observed enhancement because the effective mass of charged pions coming from its decay is predominantly outside the phase-space region where the effect is seen.

A possible contamination by η^0 meson remains around $M_{\rm inv} \sim 350$ MeV. We have performed a quantitative estimation of a possible contribution of its decay into the $\pi^+\pi^-$ subsystem using the relation between the η^0 and π^0 production cross sections. From the calculations performed by Cassing in the frame of the BUU approach [47,48] for p + Pb at 1.6 GeV the following value was found: $\sigma(\eta^0)/\sigma(\pi^0) = 4.5 \times 10^{-2}$. Assuming that the π^0 production cross section is a half of that for charged pions, the η-contribution was estimated to be about 20% of the observed correlation effect.

3.5. Nuclear shadowing effects

From the analysis performed above it follows that we observe a clear effect of positive correlations for interactions with medium and heavy targets in the region of small invariant masses, $M_{\rm inv} < 450$ MeV. This effect cannot be explained by the above considered mechanisms of non-nuclear origin. To look for a possible medium effect we have performed an additional experimental and theoretical analysis.

3.5.1. Experimental studies

To look for an absorption effect we have analyzed azimuthal correlations between emitted pions. An analysis of particle correlations in the plane perpendicular to the reaction axis has the advantage of being independent of a boost from one reference frame to another along the beam axis. Some azimuthal correlations appear naturally from a total-momentum conservation, leading particle effects etc. These types of correlations should be present mainly in elementary reactions. In nuclear interactions one can expect rather an isotropic azimuthal distribution due

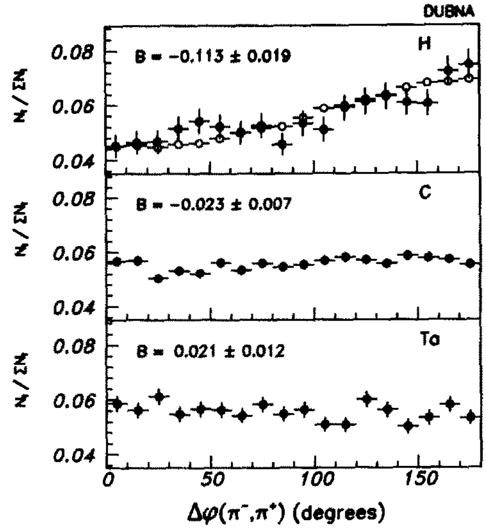

Fig. 7. Normalized distributions of the relative azimuthal angle between two pions from the Dubna data. Full circles denote the experimental distribution, open ones denote the distribution obtained from an elementary reaction $NN \to NN\pi\pi$. B denotes a value of the asymmetry coefficient defined by the formula (14).

to rescattering effects and particle production in different secondary intranuclear collisions.

To study the azimuthal $\pi\pi$ correlations we analyzed the distributions of the opening angle between the vectors of the transverse pion momenta, p_{T_i}:

$$\Delta\phi = \cos^{-1}\left(\frac{p_{T_i}\cdot p_{T_j}}{|p_{T_i}|\cdot|p_{T_j}|}\right). \tag{13}$$

The azimuthal anisotropy can be quantitatively characterized by the asymmetry coefficient defined as:

$$B = \frac{N(\Delta\phi < 90°) - N(\Delta\phi \geqslant 90°)}{N(\Delta\phi < 90°) + N(\Delta\phi \geqslant 90°)}, \tag{14}$$

where N denotes the number of pion pairs in the selected angular interval.

This method was earlier used for the analysis of the azimuthal correlations between negative pions and protons [49].

Fig. 7 and fig. 8 show the $\Delta\phi$ distributions for the pion pairs from the Dubna and Diogene data, respectively. A clear enhancement in the region of opposite pion transverse momenta for the hydrogen target is a trivial consequence of the phase-space restrictions and corresponds to the effect of negative correlations seen in the invariant-mass distribution (see fig. 3. and discussion in subsect. 3.4). For

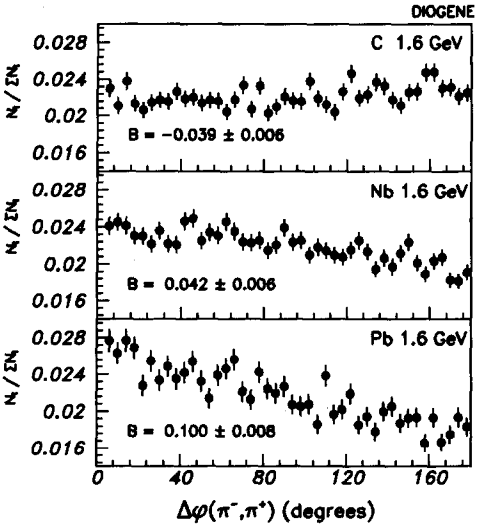

Fig. 8. Same as in fig. 7 from the Diogene data.

illustration we show in this figure an analogous distribution obtained with the phase-space simulation programme for pion pairs from the reaction NN → NN$\pi\pi$. The secondary nuclear processes introduce some randomization of different kinematical relations leading to almost isotropic azimuthal distributions seen for the carbon target both for the Dubna and Diogene data.

A qualitatively different type of correlations appears for the interactions with heavy targets. The reverse correlation effect shows a collimation of pions in the region of small $\Delta\phi$. Its strength increases with an increase of the target mass. Only weak correlations are seen for the tantalum target, however, it is not surprising as in this case several light nuclei were used (see subsect. 3.3) as a projectile which obviously leads to some averaging over the reaction plane and diminishes the correlation effect.

There exists a clear relation between the effect observed in the azimuthal correlations and the enhancement in the region of small invariant masses. A collimation of pion pairs with small opening angles in the azimuthal plane shifts the values of their invariant masses towards the low invariant-mass region due to the suppression of the number of pion pairs whose transversal momenta are opposite. It should be noted here that, in all the cases considered the distributions of $\Delta\phi$ for pions from different events are completely flat showing no azimuthal correlations.

An asymmetry in the azimuthal plane can be related to a shadowing effect which appears due to pion absorption inside nuclear matter. An influence of this mechanism on the shape of two-particle correlation function was considered theoreticaly by Gyulassy [50] and was observed experimentally in azimuthal pion

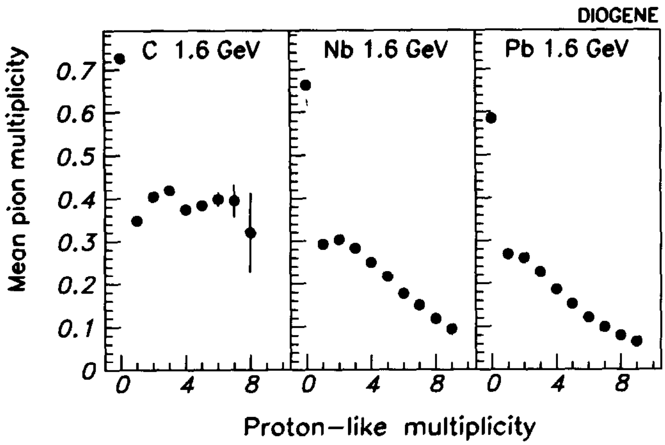

Fig. 9. The mean pion multiplicity as a function of the proton-like multiplicity from the Diogene data.

correlations by the WA80 Collaboration [51]. The importance of pion absorption was also postulated from the observation of positive transverse momentum of pions emitted from asymmetric systems at similar energies [52]. This phenomenon should clearly manifest itself in collisions of light projectiles with a heavy target as in this case pions, with transverse momenta directed towards the centre of a target nucleus, have a longer path to pass inside nuclear medium than those emitted in the opposite direction.

To verify this assumption we examined the dependence of the mean number of emitted pions on the proton-like multiplicity N_p (see subsect. 3.4) which we are using for the impact parameter selection. Fig. 9 shows this dependence for the interaction of protons with different nuclear targets (Diogene data). No clear dependence is seen for the interaction with the carbon target. A relatively large mean pion multiplicity for $N_p = 0$ is a result of the applied triggering conditions. Conversely, for the medium and heavy targets, the mean pion multiplicity decreases rapidly with the increase of N_p which can be attributed to the pion absorption inside nuclear medium.

3.5.2. *Theoretical calculations*

We have investigated the possibility that the enhancement of the correlation function close to the invariant mass of $2m_\pi$ could be caused by the effect of focussing of the two correlated pions into one hemisphere due to the presence of the target spectator matter, which causes some of the produced pions to be rescattered and absorbed. For this purpose, we performed transport calculations with the BUU code, which had been successfully used to calculate pion spectra in heavy-ion collisions [53], and to show that the observed pion collective flow [52] was caused by nuclear shadowing effects [54]. The code has recently amended following the results of ref. [55].

In our transport code we propagate protons, neutrons, Δ and N^* resonances, and pions. For their interaction cross sections, we use the experimentally measured free hadron–hadron cross sections where available. In the cases where the elementary cross sections have not been measured, we employ isospin symmetry and/or detailed balance [55] to obtain the unknown quantities. The process of greatest interest here is the creation and reabsorption of pions, which is dominated by the two-step process

$$N + N \leftrightarrow N + \Delta \leftrightarrow N + N + \pi. \tag{15}$$

In all elementary scattering processes, the medium effects of the Pauli principle on outgoing baryons are taken into account via the standard Monte Carlo rejection method. For a detailed description of the transport code see ref. [53].

In obtaining the correlation function comparable to the data, we calculate the invariant masses of correlated pions using particles from simulated events corresponding to the same impact parameter and same fixed orientation of the reaction plane. The invariant masses of background pairs are calculated taking the pair members from events at different random impact parameters and with a random relative orientation of the reaction planes. The correlation at given invariant mass M_{inv} is then computed from

$$R(M_{\text{inv}}) = \frac{\mathrm{d}N_{\text{corr}}/\mathrm{d}M_{\text{inv}}}{\mathrm{d}N_{\text{back}}/\mathrm{d}M_{\text{inv}}}, \tag{16}$$

where the subscripts "corr" and "back" refer, respectively, to the correlated and background pairs.

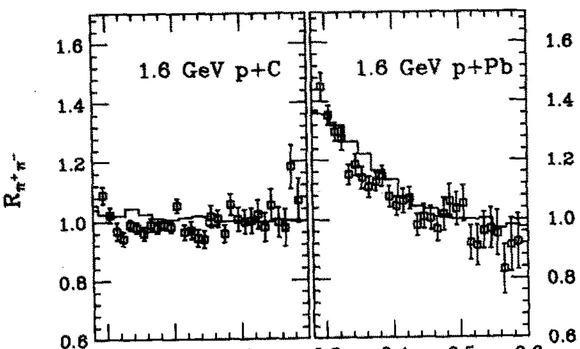

Fig. 10. A comparison of the experimental correlation function (open squares) with the theoretical calculations (histogram) for the Diogene data. See the text for details of calculations.

With the above method we approximate the experimental situation where in generating the background events one is forced to average over random relative orientations of the reaction planes and random impact parameters, while sampling the correlated pairs at one fixed orientation of the reaction plane and at one impact parameter, with the pair members focussed in the same way by spectator matter. For a more detailed description of the numerical procedure and the effect of pion absorption on two pion correlation functions see ref. [56].

In the fig. 10 we compare the results of our calculations with the experimental data for the C and Pb targets. In this case the experimental background calculations were performed without the selections of "proton-like" or "participant" numbers.

We find a satisfactory agreement with the data as well as the target mass dependence.

4. Conclusions

The analysis of $\pi^+\pi^-$ correlation in the interactions of light relativistic nuclei with light and heavy targets has been performed for the first time, using a correlation function technique. Clear positive correlations for invariant masses less than 450 MeV have been observed. The effect is strongly target dependent and increases with increasing target mass.

In order to find a source of the existing correlations the contributions of the final-state strong and Coulomb interactions between pions have been evaluated. The influence of the Coulomb interaction between a target nucleus and pions has been estimated as well. A possible contribution of the known resonance decays has been estimated for the interactions with the heaviest target.

These effects cannot explain our observations for the interactions with heavy nuclei. As a possible source of the correlations a shadowing effect due to pion absorption inside nuclear matter has been considered. Observed azimuthal correlations and transport calculations are in agreement with this assumption. Additional support comes from the analysis of the mean pion multiplicity which decreases with the decreasing impact parameter evaluated by the proton-like multiplicity. From these conclusions one can realize that the conjectured strength distribution of the σ-meson (see the Introduction) cannot be observed in the $\pi^+\pi^-$ correlations which are dominated by other medium effects. Hence, one cannot draw any conclusion about the modification of the medium corrected two-pion correlations in the nucleon–nucleon interaction.

It seems that the observed effects can be used as a test for different models of hadron–nucleus and nucleus–nucleus interactions. Taking into account a possible two-nucleon mechanism of pion absorption one can expect the absorption cross section to be dependent on the nuclear density squared [57]. Consequently, this process should take place predominantly in the central part of the nucleus and be much more sensitive to the changes of the nuclear density. Considering the pion absorption as a result of the Δ-resonance excitation/deexcitation mechanism one can expect a close connection between pion production and absorption processes.

Our observations do not exclude other possible sources of two-pion correlations. Particularly, it has been shown [58] that interference effects can also be present in the correlations of unlike pion pairs, which in principle can be used to evaluate the pion emission volume. More recently [59], new types of quantum statistical $\pi^+\pi^-$ correlations have been postulated related to the appearance of squeezed states in particle physics. To verify quantitatively different theoretical descriptions a separation of different mechanisms leading to particle correlations is highly desirable. For example a model [20] which independently considers a direct pion production and a propagation of resonance states inside nuclear medium seems to be useful for this purpose. One should also note that the effect observed by us for differently charged pions can be present as well in the case of pairs of identical pions. Thus it can affect the values of parameters extracted from the usual analysis of interference correlations of identical particles as, indeed, the effective size of the pion emission volume would be influenced by the pion absorption inside the target nucleus.

The authors are very grateful to W. Cassing for the calculation of the η^0 to π^0 production ratio. We are also grateful to our colleagues from Dubna for their participation in collecting the experimental data which we have used in the present analysis. Valuable remarks by M.I. Podgoretskii and J. Aichelin are gratefully acknowledged.

References

[1] M. Rho and D.H. Wilkinson, ed., Mesons in nuclei (North-Holland, Amsterdam, 1979)
[2] N. Hoshizaki, I. Lin and S. Machida, Prog. Theor. Phys. 26 (1961) 680;
A.E. Green and R. Sawada, Nucl. Phys. B2 (1967) 267 and references therein
[3] Particle Data Group, Phys. Lett. B50 (1974) 74;
Review of Particle Properties, Phys. Lett. B239 (1990) 1
[4] G.V. Efimov, M. Ivanov and S. Mashnik, JINR Report E2-89-780
[5] H.J. Speth, AIP Conf. Proc. on particle production near threshold, vol. 221, ed. H. Nann, E.J. Stephenson, Nashville 1990, p. 277;
J. Weinstein, ibid, p. 256
[6] D. Lohse, J.W. Durso, K. Holinde and H.J. Speth; Nucl. Phys. A516 (1990) 513
[7] P. Schuck, W. Norenberg and G. Chanfray, Z. Phys. A330 (1988) 119
[8] G. Chanfray, Z. Aouissat, P. Schuck and W. Norenberg, Phys. Lett. B256 (1991) 325
[9] V. Bernard, U.G. Meissner and I. Zahed, Phys. Rev. Lett. 59 (1987) 966
[10] M.E. Sevior, N. Grion, P. Camerini, R. Rui and D. Vetterli, Proc. Int. Workshop on pions in nuclei, Peñiscola, Spain, (3 June 1991) ed. E. Oset (World Scientific, Singapore)

[11] M. Herrmann, B.L. Friman and W. Norenberg, Z. Phys. A343 (1992) 119
[12] J.W. Durso, H.C. Kim, J. Wambach, Phys. Lett. B298 (1993) 267
[13] G. Kernel, D. Korbar, P. Križan, M. Mikuž, P. Sever, A. Stanovnik, M. Starič, D. Zavrtanik, E.G. Michaelis, N.W. Tanner, C.W.E. van Eijk, R.W. Hollander, W. Lourens, S.A. Clark, J.D. Davies, J. Lowe, S.M. Playfer and J.V. Jovanovich, Z. Phys. C51 (1991) 377 and references therein
[14] K. Wehrberger and R. Wittman, Nucl. Phys. A513 (1990) 603
[15] B. ter Haar and R. Malfliet, Phys. Rev. C36 (1987) 1611
[16] D.V. Bugg, A.J. Oxley, J.A. Zoll, J.G. Rushbrooke, V.E. Barnes, J.B. Kinson, W.P. Dodd, G.A. Doran and L. Riddiford, Phys. Rev. 133 (1964) B1017
[17] A.M. Eisner, E.L. Hart, R.I. Loutit and T.W. Morris, Phys. Rev. 138 (1965) B670
[18] R. Stock, Phys. Reports 135 (1986) 261
[19] J. Cugnon, Nucl. Phys. A462 (1987) 751
[20] Y. Pang, T.J. Schlagel and S.H. Kahana, Phys. Rev. Lett. 68 (1992) 2743
[21] J. Cugnon and M.C. Lemaire, Nucl. Phys. A489 (1988) 781
[22] M. Trzaska and Diogene Collaboration, Z. Phys. A340 (1991) 325
[23] M.C. Lemaire and Diogene Collaboration, Phys. Rev. C43 (1991) 2711
[24] V.G. Ableev, S.M. Eliseev, V.I. Inozemtsev, B. Naumann, L. Naumann, A.A. Nomofilov, N.M. Piskunov, I.M. Sitnik, E.A. Strokovsky, L.N. Strunov, V.I. Sharov and S.A. Zaporozhets, JINR Report E1-87-797
[25] I. Angelov, A.I. Anoshin, N. Akhababyan, C. Baatar, A.M. Baldin, J. Bartke, S. Backovic, A.N. Gasparyan, N.S. Grigalashvili, V.G. Grishin, S.V. Dzhmukhadze, L.A. Didenko, I.A. Ivanovskaya, L. Jenik, T. Kanarek, E.P. Kladnitskaya, D.K. Kopylova, V.B. Lyubimov, N.N. Melnikova, V.F. Nikitina, V.M. Popova, S.I. Lyutov, A.N. Solomin, M.I. Solovyov, M.K. Suleymanov, G.P. Toneeva, D. Tuvdendorzh, A.P. Tcheplakov, A.I. Shklovskaya, L.M. Scheglova, E.O. Abdurakhmanov, A.N. Basina, A.H. Vinitskij, A.Sh. Gaytinov, I.S. Streltsov, I.Ya. Tchasikov, O.B. Abdipov, T. Gomoshi, Sh. Krasnovsky, E. Balea, O. Balea, V. Bodea, S. Felea, T. Ponta, D. Armutlijski, S. Prokopyeva, E. Bialkowska, L. Zurawik, D. Kieliczewska, I.M. Agagabyan, V.A. Vartanyan, G.R. Gulkanyan, Z.A. Kirakosyan, S.A. Korchagin, M. Kowalski, I.P. Erofeeva, V.S. Murzin, L.P. Smirnova, Z. Korbiel, Z. Trka, J. Trkova, P. Kerachev, P. Markov, H.R. Samerdzhiev, S.A. Azimov, Sh.V. Inogamov, K.T. Turdalyov, A.A. Yuldashev, B.S. Yuldashev, I.S. Amaglobeli, T.G. Makharadze, Yu.V. Tevzadze, M.V. Topuridze, E.T. Tsivtsivadze, H. Dalkhazhav, B. Tchadraa and P. Togoo, Yad. Fiz. 30 (1979) 1590 [Sov. J. Nucl. Phys. 30 (1979) 824]
[26] G.N. Agakishiev, N. Akhababyan, Ts. Baatar, A.M. Baldin, E. Balea, O. Balea, E. Bartke, E. Bialkovska, E. Bogdanovich, V. Boldea, A.P. Gasparyan, N.S. Grigalashvili, V.G. Grishin, K.K. Gudima, L.D. Didenko, I.A. Ivanovskaya, T. Kanarek, R.A. Kvatadze, E.N. Kladnitskaya, M. Kowalski, E. Kondor, D.K. Kopylova, V.B. Lyubimov, R.R. Mekhtiev, V.F. Nikitina, T. Ponta, V.M. Popova, L. Simic, M.I. Solovev, A.N. Solomin, M.K. Suleimanov, G.P. Toneeva, V.D. Toneev, S. Khakman, A.P. Cheplakov and L.M. Shcheglova, Yad. Fiz. 37 (1983) 938 [Sov. J. Nucl. Fiz. 37 (1983) 559]
[27] J.P. Alard and Diogene Collaboration, Nucl. Instr. Meth. A261 (1987) 379
[28] Lj. Simić, S. Backović, H. Agakishiev, V.G. Grishin, T. Kanarek, E.N. Kladnitskaya, V. Boldea and S. Ditza, Phys. Rev. D34 (1986) 692
[29] G.N. Agakishiev, T. Kanarek, E.N. Kladnitskaya, N.I. Kotchnev, V.M. Popova, S.Yu. Sivoklokov, G.P. Toneeva and A.P. Tcheplakov, JINR Report 1-83-662
[30] W.A. Zajc, J.A. Bistirlich, R.R. Bossingham, H.R. Bowman, C.W. Clawson, K.M. Crowe, K.A. Frankel, J.G. Ingersoll, J.M. Kurck, C.J. Martoff, D.L. Murphy, J.O. Rasmussen, J.P. Sullivan, E. Yoo, O. Hashimoto, M. Koike, W.J. McDonald, J.P. Miller and P. Truöl, Phys. Rev. C29 (1984) 2173
[31] M. Arneodo and the European Muon Collaboration, Z. Phys. C32 (1986) 1
[32] A.D. Chacon, J.A. Bistirlich, R.R. Bossingham, H. Bossy, H.R. Bowman, C.W. Clawson, K.M. Crowe, T.J. Humanic, M. Justice, P. Kammel, J.M. Kurck, S. Ljungfelt, C.A. Meyer, C. Petitjean, J.O. Rasmussen, M.A. Stoyer, O. Hashimoto, Wm.C. McHarris, J.P. Sullivan, K.L. Wolf and W.A. Zajc, Phys. Rev. C43 (1991) 2670
[33] D. Drijard, H.G. Fischer and T. Nakada, Nucl. Instr. Meth. 225 (1984) 367

[34] Lj. Simić, S. Backović, H. Agakishiev, V.G. Grishin, T. Kanarek, E.N. Kladnitskaya, V. Boldea and S. Ditza, Phys. Rev. C37 (1988) 2064
[35] M. Gyulassy and S.K. Kauffmann, Nucl. Phys. A362 (1981) 503
[36] R. Lednicky and V.L. Lyuboshitz, Yad. Fiz. 35 (1982) 1316 [Sov. J. Nucl. Phys. 35 (1982) 770]
[37] M. Gmitro, J. Kvasil, R. Lednicky and V.L. Lyuboshitz, Czech. J. Phys. B36 (1986) 1281
[38] N.A. Kalinina and R. Lednicky, private communication
[39] M.M. Nagels, Nucl. Phys. B147 (1979) 189
[40] E.A. Alekseeva, A.A. Kartamyshev, V.K. Makar'in, K.N. Mukhin, O.O. Patarakin, M.M. Sulkovskaya, A.F. Sustavov, L.V. Surkova and L.A. Chernysheva, Zh. Eksp. Teor. Fiz. 82 (1982) 1007
[41] J.D. Jackson and J.O. Blatt, Rev. Mod. Phys. 22 (1950) 77
[42] B.M. Bobchenko, A.E. Buklei, A.V. Vlasov, I.I. Vorobyev, L.S. Vorobyev, N.A. Goryainov, Yu.G. Grishuk, O.B. Guschin, B.L. Druzhinin, V.V. Zhurkin, G.N. Zavrazhanov, M.V. Kosov, G.A. Leksin, V.L. Stolin, V.P. Surin, V.B. Fedorov, B.A. Fominykh, B.B. Shvartzman, S.V. Shevchenko and S.M. Shuvalov, Yad. Fiz. 30 (1979) 1553
[43] J. Bartke, Phys. Lett. B174 (1986) 32
[44] G.N. Agakishiev, D. Armutlijski, N. Akhababyan, J. Bartke, J. Bogdanowicz, A.P. Gasparyan, N.S. Grigalashwili, V.G. Grishin, L.A. Didenko, I.A. Ivanovskaya, T. Kanarek, E.N. Kladnitskaya, M. Kowalski, D.K. Kopylova, V.B. Lyubimov, Z.V. Metreveli, R.R. Mekhtiev, V.F. Nikitina, V.M. Popova, M.I. Solovyov, A.N. Solomin, G.P. Toneeva, A.P. Tcheplakov, and L.M. Scheglova, Yad. Fiz. 39 (1984) 543
[45] G.N. Agakishiev et al., Yad. Fiz. 39 (1984) 543
[46] T. Akesson and the Axial Field Spectrometer Collaboration, Z. Phys. C36 (1987) 517
[47] A. De Paoli, K. Niita, W. Cassing, U. Mosel and C.M. Ko, Phys. Lett. B219 (1989) 194
[48] W. Cassing, V. Metag, U. Mosel and K. Niita, Phys. Reports 188 (1990) 365;
W. Cassing, private communication
[49] Lj. Simić, S. Backović, H.N. Agakishiev, E.N. Kladnitskaya and A.P. Cheplakov, Phys. Rev. C45 (1992) 2417
[50] M. Gyulassy, Phys. Rev. Lett. 48 (1982) 454
[51] H.R. Schmidt and WA80 Collaboration, Nucl. Phys. A544 (1992) 449c
[52] J. Gosset and Diogene Collaboration, Phys. Rev. Lett. 62 (1989) 1251
[53] B.A. Li and W. Bauer, Phys. Rev. C44 (1991) 450
[54] B.A. Li, W. Bauer and G.F. Bertsch, Phys. Rev. C44 (1991) 2095
[55] P. Danielewicz and G.F. Bertsch, Nucl. Phys. A533 (1991) 712
[56] D. Klakow, W. Bauer, P. Danielewicz and P. Schuck, in preparation
[57] D.A. Sparrow and M.M. Sternheim, Phys. Rev. C10 (1974) 2215
[58] S.S. Kozlovska and M.I. Podgoretskii, Yad. Fiz. 24 (1976) 621;
M.I. Podgoretskii, Part. Nucl. 20 (1989) 628
[59] I.V. Andreev, M. Plumer, R.M. Weiner, to be published;
R.M. Weiner, private communication